BRITE EURAM III

INDUSTRIAL DEMONSTRATION OF ACCURATE AND EFFICIENT MULTIDIMENSIONAL UPWIND AND MULTIGRID ALGORITHMS FOR AERODYNAMIC SIMULATION ON UNSTRUCTURED GRIDS (IDeMAS)

February 1999

TECHNICAL REPORT

N^{O} TR 7.1.1

Implementation of MDHR for Euler in industrial environment (Task 7.1.1). Period: 01/01/1998 to 31/12/1998

J.Bastin and G.Rogé (Dassault)

Partners

von Karman Institute
Inst. Nat. de R. en Informatique et en Automatique
C. di Ricerca, Sviluppo e Studi Superiori in Sardegna
Ecole Polytechnique Fédérale de Lausanne
Dassault Aviation
Daimler-Chrysler Aerospace
Alenia Aerospazio

TECHNICAL REPORT

Contract N^{o} : BRPR-CT97-0591

Project N^{o} : BE97-4162

Title : INDUSTRIAL DEMONSTRATION OF ACCURATE AND EFFICIENT MULTIDIMENSIONAL UPWIND AND MULTIGRID ALGORITHMS FOR AERODYNAMIC SIMULATION ON UNSTRUCTURED GRIDS (IDeMAS)

Project Coordinator : von Karman Institute

Partners :
von Karman Institute
Inst. Nat. de R. en Informatique et en Automatique
C. di Ricerca, Sviluppo e Studi Superiori in Sardegna
Ecole Polytechnique Fédérale de Lausanne
Dassault Aviation
Daimler-Chrysler Aero.
Alenia Aerospazio

Period : from 01/01/1998 **to** 31/12/1998

Report N^{o} : TR 7.1.1

Starting date : 01/01/1998

Duration : 36 months

Date of issue of this report : February 1999

Project funded by the European Community under the Industrial & Materials Technologies Programme (BRITE/EURAM III)

Index

1 Summary

The fluctuation splitting schemes have been introduced by P.L.Roe at the beginning of the 80's and have been then developed until now, essentially thanks to H.Deconinck. In this paper, the fluctuation splitting schemes formalism is recalled. Then, the hyperbolic elliptic decomposition of the three dimensional Euler equations is presented. This decomposition leads to an acoustic subsystem and two scalar advection equations, one of them being the entropy advection. Thanks to this decomposition, the two scalar equations are treated with the well known scalar fluctuation splitting scheme, the PSI one, and the acoustic subsystem is treated with a matrix fluctuation splitting scheme, the Lax Wendroff scheme. Moreover, an additional viscous term is introduced in order to reduce the oscillatory behavior of the Lax Wendroff scheme. An important work about the implicitation of this scheme allow then to obtain a robust scheme which allows computations within a large range of validity, in terms of Mach number. This fluctuation splitting scheme, called the Lax Wendroff - PSI scheme, allows to reduce the spurious entropy and then to compute drags more precisely. At the end, numerical results obtained with this Lax Wendroff PSI scheme are shown and compared to a reference Euler code, based on a Lax Wendroff scheme.

2 Introduction

The computation of the non-viscous flow over an entire aircraft configuration with unstructured meshes is a fairly routine task for Dassault Aviation.

Among the applications of the computations, we can mention definition of design loads and flutter analysis. Another application is to check that the shocks are not dangerously located for the stability of the aircraft or for the functionning of the engines. About this last point, the position of the shocks are obtained by coupling the Euler computations with a boundary layer code. For all these applications, numerical accuracy is needed, especially for aerodynamic coefficients, locations of the shocks and, in a weaker way, for the pressure distribution along the aircraft.

Our industrial constraints are first to have a large range of validity in terms of Mach number because Dassault Aviation may compute both low subsonic flows and nearly hypersonic ones. Another wish is to have a code which is not computation-case dependent. Of course, reliability, robustness and reasonnable cpu cost are also needed.

Despite a lot of research and development activity that has led to accurate and robust formulations during the 80's, need for further progress is still identified. For instance, the absolute value of the drag is still not always predicted with enough accuracy, due to spurious entropy production.

In this context, Dassault Aviation is always trying to get more accurate or more robust for-

mulations. Recently, around 95 [2], the development of the fluctuation splitting schemes have shown that such formulations are now accessible. More precisely, the works dealing with the fluctuation splitting schemes have shown that numerical schemes with a low numerical entropy are possible.

In this paper, after a general presentation of the fluctuation splitting schemes, we present the fluctuation splitting scheme we have implemented in the industrial Euler code of Dassault Aviation and the numerical results we have got with this scheme.

3 The fluctuation splitting schemes

3.1 The fluctuation splitting formalism

These new kind of numerical schemes have been initiated by Roe in 1982 and have been developed by many others. The fluctuation splitting schemes, also called residual distribution schemes, have been largely presented in the litterature, for instance in Deconinck and al. 93 [1] or in Paillère 95 [2].

We recall here the fluctuation splitting methodology for solving the scalar conservation law problem on an arbitrary triangulation of a domain Ω.

We consider the problem

$$\begin{cases} \dfrac{\partial u}{\partial t} + \nabla \cdot \vec{F} = 0 \quad \forall\ (x,y,z) \in \Omega,\ \forall\ t > 0 \\ \text{Boundary conditions} \\ \text{Cauchy conditions} \end{cases} \tag{1}$$

Just like in linear finite element methods, the solution is approximated by a continuous function, varying linearly over each tetrahedra,

$$u(x,y,z,t) = \sum_i u_i(t)\omega_i(x,y,z) \tag{2}$$

where $u_i(t)$ is the value of u at node i, and ω_i the linear shape function equal to unity at (x_i, y_i, z_i) and equal to zero outside the support of all tetrahedra meeting at node i.

The integration over an element T leads to

$$\iiint_T \frac{\partial u}{\partial t} dV = -\iiint_T \vec{\lambda} \cdot \nabla u \ dV \tag{3}$$

where we have noted

$$\vec{\lambda} = \frac{\partial \vec{F}}{\partial u} \tag{4}$$

With a first order in time approximation, we can write the left hand side of the equation 3 in the local element numering as

$$\iiint_T \frac{\partial u}{\partial t} dV = \frac{V_T}{4}\left[\frac{u_1^{n+1}-u_1^n}{\Delta t}+\frac{u_2^{n+1}-u_2^n}{\Delta t}+\frac{u_3^{n+1}-u_3^n}{\Delta t}+\frac{u_4^{n+1}-u_4^n}{\Delta t}\right] \tag{5}$$

where V_T denotes the volume of the element T.

For the right hand side, we choose an approximation in order to compute the residual $\Phi^T = \int_T \vec{\lambda}\cdot\nabla u \; dV$. The idea of the fluctuation splitting schemes is then to split the residual in

$$\Phi^T = \Phi_1^T + \Phi_2^T + \Phi_3^T + \Phi_4^T \tag{6}$$

The fluctuation splitting method consists of distributing fractions of the residual. This leads to the explicit scheme

$$\sum_{T\ tq\ i\in T} \frac{V_T}{4}\frac{u_i^{n+1}-u_i^n}{\Delta t} = -\sum_{T\ tq\ i\in T} \Phi_i^T \tag{7}$$

or, in an equivalent way,

$$u_i^{n+1} = u_i^n - \frac{\Delta t}{V_i}\sum_T \Phi_i^T \tag{8}$$

after having introduced $V_i = \sum_{T\ tq\ i\in T} \frac{V_T}{4}$ which is no more than the volume of the dual cell at node i.

It is often useful to introduce the β_i^T defined by $\Phi_i^T = \beta_i^T \Phi^T$. We require that $\sum_{i\in T}\beta_i = 1$ for consistency.

Fluctuation splitting schemes were usually first developped for the scalar advection equation. Then, the problem of the extension of the scalar schemes to systems has to be solved.

This problem is easily solved when the system is diagonalisable. In this case, scalar schemes can be used for each scalar equations of the diagonalised system. But, here, our aim is to solve Euler equations, which are not diagonalisable.

For such not diagonalisable systems, two main orientations are identified. One consists of a formal extension of the scalar scheme. An application of this idea is done for the N-scheme (Narrow scheme) in Bonfiglioli and al. 96 [3]. The other orientation, first introduced by Roe in 1986 [4], is to decompose the initial residual Φ_T as a sum of simple wave solutions.

3.2 The properties of the distributions

We recall here the main properties of the fluctuation splitting schemes and the conditions they impose on the distributions Φ_i^T.

Before listing these properties, we need to introduce, for each node i of an element T, $k_i = \frac{1}{3}\vec{\lambda}\cdot\vec{n}_i$ with $\vec{n}_i$ the interior normals to the tetrahedra T, pointed toward the node i, scaled by their respective surfaces. Thus, one has $\sum_{i=1}^{4}\vec{n}_i = \vec{0}$ and $\sum_{i=1}^{4} k_i = 0$.

First, a fluctuation splitting scheme is said to be upwind when the distributions Φ_i^T satisfy

$$(\mathcal{U}) \quad \beta_i^T = 0 \text{ if } k_i < 0 \tag{9}$$

This property is called upwinding because it is the exact extension of the upwinding notion for the resolution of the one dimensional convection equation.

Another property is positivity. A fluctuation splitting scheme is said to be positive if the value at the new time-step can be written as a convex sum of values at the previous time-step,

$$(\mathcal{P}) \quad u_i^{n+1} = \sum_k c_k u_k^n \text{ with } c_k \geq 0 \ \forall k \tag{10}$$

together with the consistency condition $\sum_k c_k = 1$.

The last important property is linearity preserving. This property is strongly tied to second order accuracy. A fluctuation splitting scheme is said to be linearity preserving when

$$(\mathcal{LP}) \quad \Phi_i^T \to 0 \text{ when } \Phi^T \to 0 \tag{11}$$

a sufficient condition to guaranty this property being that β_i^T is bounded.

Before going on, we have to precise how we take into account the boundary conditions.

3.3 The boundary conditions

We choose a treatment of the boundary conditions which allow us to use all the subroutines which have been written for our finite volume schemes, for instance those of our reference code.

The finite volume schemes lead to the decomposition

$$\begin{aligned} \int_\Omega \phi W_t &= -\int_\Omega \nabla\cdot\mathcal{F}\phi \\ &= \int_\Omega \mathcal{F}\nabla\phi - \int_{\partial\Omega}\phi\mathcal{F}\cdot\vec{n} \end{aligned} \tag{12}$$

where ϕ is a test function. Then a weak formulation of boundary conditions is used to compute $\int_{\partial\Omega}\phi\mathcal{F}\cdot\vec{n}$.

In the fluctuation splitting formalism, $\int_\Omega \nabla\cdot\mathcal{F}\phi$ is directly computed. In order to make the same treatment as in the finite volume case, we write

$$\begin{aligned} \int_\Omega \phi W_t &= -\int_\Omega \mathcal{A}\nabla W\phi \\ &= -\int_\Omega \mathcal{A}\nabla W\phi + \int_{\partial\Omega}\phi\mathcal{F}\cdot\vec{n} - \int_{\partial\Omega}\phi\mathcal{F}\cdot\vec{n} \end{aligned} \tag{13}$$

Thus, we compute in a first time

$$\underbrace{-\iiint_\Omega \mathcal{A}\nabla W\phi}_{\text{fluctuation splitting}} \quad + \quad \underbrace{\iint_{\partial\Omega} \phi\mathcal{F}\cdot\vec{n}}_{\text{centered treatment}} \tag{14}$$

and then we add $\int_{\partial\Omega}\phi\mathcal{F}\cdot\vec{n}$, which we compute with a weak formulation of the boundary conditions.

4 A crucial decomposition of the Euler equations

In this section, we recall the hyperbolic elliptic decomposition of the Euler equations. This decomposition, which is inspired by the Deconinck-Hirsch decomposition [5], has been exposed in Paillère 95 [2] in the two dimensional case and in Bonfiglioli and al. 96 [3] in the three dimensional case. This decomposition is a crucial point for the scheme we are going to deal with in the next section.

The Euler equations are usually written with a conservative form using the variable

$$W = \begin{pmatrix} \rho \\ \rho u \\ \rho v \\ \rho w \\ \rho e \end{pmatrix} \tag{15}$$

where ρ represents the gas density, u, v and w are the $x-$, $y-$ and $z-$ components of the velocity vector $\vec{u}$, e is the specific total energy and h the specific total enthalpy.

This conservative form is

$$\frac{\partial F}{\partial x} + \frac{\partial G}{\partial y} + \frac{\partial H}{\partial z} = 0 \tag{16}$$

with

$$F = \begin{pmatrix} \rho u \\ \rho u^2 + p \\ \rho uv \\ \rho uw \\ \rho uh \end{pmatrix}, G = \begin{pmatrix} \rho v \\ \rho uv \\ \rho v^2 + p \\ \rho vw \\ \rho vh \end{pmatrix}, H = \begin{pmatrix} \rho w \\ \rho uw \\ \rho vw \\ \rho w^2 + p \\ \rho wh \end{pmatrix} \tag{17}$$

and we note

$$\mathcal{F} = F\vec{1}_x + G\vec{1}_y + H\vec{1}_z \tag{18}$$

In the fluctuation splitting context, it is useful to consider the quasi linear form of the Euler equations

$$A\frac{\partial W}{\partial x} + B\frac{\partial W}{\partial y} + C\frac{\partial W}{\partial z} = 0 \tag{19}$$

with

$$A = \frac{\partial F}{\partial W} \ , \ B = \frac{\partial G}{\partial W} \ , \ C = \frac{\partial H}{\partial W} \tag{20}$$

and we note

$$\mathcal{A} = A\vec{1}_x + B\vec{1}_y + C\vec{1}_z \tag{21}$$

Although we want to solve the steady Euler equations, we will consider the unsteady Euler equations because we use a pseudo unsteady process with local time-stepping to reach steady states. Thus, we consider

$$\frac{\partial W}{\partial t} + A\frac{\partial W}{\partial x} + B\frac{\partial W}{\partial y} + C\frac{\partial W}{\partial z} = 0 \tag{22}$$

Two changes of variables have to be made in order to obtain the hyperbolic elliptic decomposition.

In a first step, we use the symmetrizing variables:

$$\partial Q = \begin{pmatrix} \dfrac{\partial p}{\rho a} \\ \partial u \\ \partial v \\ \partial w \\ \partial p - a^2 \partial \rho \end{pmatrix} = M \partial V \text{ with } V = \begin{pmatrix} \rho \\ u \\ v \\ w \\ p \end{pmatrix} \text{ and } M = \begin{bmatrix} 0 & 0 & 0 & 0 & 1/\rho a \\ 0 & 1 & 0 & 0 & 0 \\ 0 & 0 & 1 & 0 & 0 \\ 0 & 0 & 0 & 1 & 0 \\ -a^2 & 0 & 0 & 0 & 1 \end{bmatrix} \tag{23}$$

where we note a the velocity of sound and p the pressure.

With the variable Q, the Euler equations become

$$\frac{\partial Q}{\partial t} + \tilde{A}\frac{\partial Q}{\partial x} + \tilde{B}\frac{\partial Q}{\partial y} + \tilde{C}\frac{\partial Q}{\partial z} = 0 \tag{24}$$

with

$$\tilde{A} = \begin{bmatrix} u & a & 0 & 0 & 0 \\ a & u & 0 & 0 & 0 \\ 0 & 0 & u & 0 & 0 \\ 0 & 0 & 0 & u & 0 \\ 0 & 0 & 0 & 0 & u \end{bmatrix}, \tilde{B} = \begin{bmatrix} v & 0 & a & 0 & 0 \\ 0 & v & 0 & 0 & 0 \\ a & 0 & v & 0 & 0 \\ 0 & 0 & 0 & v & 0 \\ 0 & 0 & 0 & 0 & v \end{bmatrix} \text{ and } \tilde{C} = \begin{bmatrix} w & 0 & 0 & a & 0 \\ 0 & w & 0 & 0 & 0 \\ 0 & 0 & w & 0 & 0 \\ a & 0 & 0 & w & 0 \\ 0 & 0 & 0 & 0 & w \end{bmatrix} \tag{25}$$

After this symmetrization of the Euler equations, we introduce the second change of variables

$$\partial \tilde{W} = \begin{pmatrix} \dfrac{\beta}{\rho a}\partial p + M\vec{s}\cdot\partial\vec{u} \\ \dfrac{\beta}{\rho a}\partial p - M\vec{s}\cdot\partial\vec{u} \\ M\vec{t}\cdot\partial\vec{u} \\ \dfrac{\partial p}{\rho a} + M\vec{n}\cdot\partial\vec{u} \\ \partial p - a^2\partial\rho \end{pmatrix} = \check{L}\partial Q \text{ with } \check{L} = \begin{bmatrix} \beta & Ms_x & Ms_y & Ms_z & 0 \\ \beta & -Ms_x & -Ms_y & -Ms_z & 0 \\ 0 & Mt_x & Mt_y & Mt_z & 0 \\ 1 & Mn_x & Mn_y & Mn_z & 0 \\ 0 & 0 & 0 & 0 & 1 \end{bmatrix} \tag{26}$$

where we have noted $\vec{n} = \dfrac{\vec{u}}{\| \vec{u} \|}$ and we have taken $\left(\vec{n}, \vec{s}, \vec{t}\right)$ as an orthonormal direct base.

This change of variables leads to

$$\frac{\partial W}{\partial t} + \frac{\partial W}{\partial Q}\left[\tilde{A}\check{R}\frac{\partial \tilde{W}}{\partial x} + \tilde{B}\check{R}\frac{\partial \tilde{W}}{\partial y} + \tilde{C}\check{R}\frac{\partial \tilde{W}}{\partial z}\right] = 0 \tag{27}$$

with $\check{R} = \check{L}^{-1}$.

In order to obtain the hyperbolic elliptic decomposition, we have to use the preconditionning matrix which Van Leer and al. introduced in 91 [6] and which was extended to the 3D case by Bonfiglioli and al. in 96 [3]

$$\tilde{P} = \frac{1}{q}\begin{bmatrix} \dfrac{\chi M^2}{\beta^2} & \dfrac{-\chi M u}{\beta^2 q} & \dfrac{-\chi M v}{\beta^2 q} & \dfrac{-\chi M w}{\beta^2 q} & 0 \\ \dfrac{-\chi M u}{\beta^2 q} & \eta\dfrac{u^2}{q^2} + \chi & \eta\dfrac{uv}{q^2} & \eta\dfrac{uw}{q^2} & 0 \\ \dfrac{-\chi M v}{\beta^2 q} & \eta\dfrac{uv}{q^2} & \eta\dfrac{v^2}{q^2} + \chi & \eta\dfrac{vw}{q^2} & 0 \\ \dfrac{-\chi M w}{\beta^2 q} & \eta\dfrac{uw}{q^2} & \eta\dfrac{vw}{q^2} & \eta\dfrac{w^2}{q^2} + \chi & 0 \\ 0 & 0 & 0 & 0 & 1 \end{bmatrix} \tag{28}$$

with $q = \| \vec{u} \|$ and β, χ and η defined as

$$\beta = \sqrt{\max\left(\varepsilon^2, \mid M^2 - 1 \mid\right)},\ \chi = \frac{\beta}{\max\left(M, 1\right)} \text{ and } \eta = \frac{\chi + \beta^2}{\beta^2} - \chi \tag{29}$$

with $\epsilon = 0.05$, like in Paillère 95 [2].

With this matrix, we write equation 27 in an equivalent form

$$\frac{\partial W}{\partial t} + \frac{\partial W}{\partial Q}\tilde{P}^{-1}\check{R}\left[\check{L}\tilde{P}\tilde{A}\check{R}\frac{\partial \tilde{W}}{\partial x} + \check{L}\tilde{P}\tilde{B}\check{R}\frac{\partial \tilde{W}}{\partial y} + \check{L}\tilde{P}\tilde{C}\check{R}\frac{\partial \tilde{W}}{\partial z}\right] = 0 \tag{30}$$

This new form leads to

$$\frac{\partial W}{\partial t} + \frac{\partial W}{\partial Q}P^{-1}\check{R}\mathcal{R}\left(\check{W}\right) = 0 \tag{31}$$

with

$$\mathcal{R}\left(\check{W}\right) = \begin{bmatrix} \chi\nu^+\vec{n} + \dfrac{\chi}{\beta}\vec{s} & \chi\nu^-\vec{n} & \dfrac{\chi}{\beta}\vec{t} & 0 & 0 \\ \chi\nu^-\vec{n} & \chi\nu^+\vec{n} - \dfrac{\chi}{\beta}\vec{s} & \dfrac{\chi}{\beta}\vec{t} & 0 & 0 \\ \dfrac{\chi}{2\beta}\vec{t} & \dfrac{\chi}{2\beta}\vec{t} & \chi\vec{n} & 0 & 0 \\ 0 & 0 & 0 & \vec{n} & 0 \\ 0 & 0 & 0 & 0 & \vec{n} \end{bmatrix} \cdot \nabla\check{W} \text{ and } \nu^{\pm} = \frac{M^2 - 1 \pm \beta^2}{2\beta^2} \tag{32}$$

Thus, we have obtained an equivalent form of the Euler equations (eq 31), at least locally over each element T.

In this new form, two different parts can be distinguished. The three first equations of the equation 32 constitute a subsystem which is independent of the two last equations and is called the acoustic subsystem. The two last ones are entirely decoupled scalar advection equations.

Upon this decompostion, we can treat the two parts in different ways. This is the object of the next section, where we introduce the Lax Wendroff - PSI scheme.

5 The Lax Wendroff - PSI scheme

We present here the Lax Wendroff - PSI scheme. This scheme is based upon the matrix-scalar decompostion of the residual. Indeed, the divergence of the fluxes can be written as the sum of the residual of the acoustic subsystem and of the residuals of the last two scalar advection equations:

$$\frac{\partial F}{\partial x}+\frac{\partial G}{\partial y}+\frac{\partial H}{\partial z}=\underbrace{\left(r^1,r^2,r^3\right)\left[a\cdot\nabla\begin{pmatrix}\check{W}^1\\ \check{W}^2\\ \check{W}^3\end{pmatrix}\right]}_{\Phi_{coupled}}+\underbrace{\vec{\lambda}^4\cdot\check{W}^4r^4}_{\Phi_{enthal}}+\underbrace{\vec{\lambda}^5\cdot\check{W}^5r^5}_{\Phi_{entrop}} \tag{33}$$

where we have noted r^i the vectors of the matrix $\dfrac{\partial W}{\partial Q}P^{-1}\check{R}$, $\vec{\lambda}^l$ the advection vectors of the last two scalar equations (in practise, $\vec{\lambda}^4=\vec{\lambda}^5=\vec{n}$) and

$$a=\begin{bmatrix}\chi\nu^+\vec{n}+\dfrac{\chi}{\beta}\vec{s} & \chi\nu^-\vec{n} & \dfrac{\chi}{\beta}\vec{t}\\ \chi\nu^-\vec{n} & \chi\nu^+\vec{n}-\dfrac{\chi}{\beta}\vec{s} & \dfrac{\chi}{\beta}\vec{t}\\ \dfrac{\chi}{2\beta}\vec{t} & \dfrac{\chi}{2\beta}\vec{t} & \chi\vec{n}\end{bmatrix}=(a_x,a_y,a_z) \tag{34}$$

The strategy of the Lax Wendroff - PSI scheme (LW-PSI scheme) is to split the acoustic residual, $\Phi_{coupled}$, with a matrix fluctuation splitting and the two scalar residuals, Φ_{enthal} and Φ_{entrop} with a scalar fluctuation splitting scheme.

In the LW-PSI scheme, the matrix Lax Wendroff scheme is used to split $\Phi_{coupled}$ and the PSI scheme is used to split Φ_{enthal} and Φ_{entrop}.

5.1 The matrix Lax Wendroff scheme

The Lax Wendroff scheme can be formulated as a fluctuation splitting scheme, as shown by Roe in 87 [7]. Thus, in the scalar case, the Lax Wendroff scheme corresponds to the distribution

$$\beta_i^{LW,T} = \frac{1}{4} + \frac{\Delta t}{2V^T} k_i \tag{35}$$

The matrix Lax Wendroff scheme is obtained with a formal generalisation of equation 35. Thus, we have

$$\beta_i^{LW,T} = \frac{1}{4} Id + \frac{\Delta t}{2V^T} K_i \tag{36}$$

where K_i is a matrix generalisation of the scalar k_i

$$K_i = \frac{1}{3} \left[a_x \; n_{i_x} + a_y \; n_{i_y} + a_z \; n_{i_z} \right] \tag{37}$$

The Rudgyard extension of the time-step [8] [9] allows us to get a matrix Lax Wendroff scheme where Δt does not appear any longer:

$$\beta_i^{LW,T} = \frac{1}{4} Id + \frac{\nu_{cell}}{2} K_i \left(\sum_j \mid K_j \mid \right)^{-1} \tag{38}$$

where ν_{cell} is a constant taken to 1 and $\mid K_i \mid$ is the matrix which has the same eigenvectors as K_i but whose eigenvalues are the absolute value of those of K_i.

5.2 The PSI scheme

The PSI (Positive Streamwise Invariant) scheme has been introduced by Strujis and al. in 91 [10]. In 95, Sidilkover and al. [11] showed that this PSI scheme can be obtained by applying the Min Mod limiter function to the N-scheme. The Min Mod limiter function is exposed in [12], and the N-scheme is a very popular fluctuation splitting scheme to which Sildikover gave its name in 89 [13]. This former scheme has been well extended to the three dimensional case by Bonfiglioli and al. in 96 [3].

This scheme is a scalar upwinding fluctuation splitting scheme which is positive and linearity preserving. These properties make this scheme one of the most performant one to solve the scalar advection problem. The handicap of this scheme is that it can not be extended to the system case in a satisfactory way.

This scheme could be replaced, in two dimensions, by the N-SUPG scheme of R.Abgrall (private communication). As far as numerical results are concerned, all the two dimensions test cases give same results whether the PSI scheme or the N-SUPG scheme is used.

5.3 An additional viscous term

The first uses of the LW-PSI scheme showed an oscillatory behavior in two dimensions. In three dimensions, this behavior became a main obstacle for computations. For instance, a pure

subsonic computational case over a wing could not be realized with this scheme as soon as Mach number was higher than 0.5.

As a matter of fact, this behavior is not surprising because we use a Lax Wendroff scheme to split the acoustic residual, and it is well known that the Lax Wendroff scheme is not monotone and generates oscillations near the shocks.

In order to reduce this oscillatory behavior, we add a viscous term to the LW-PSI scheme. This term is based on the second order term which can be found in the Peraire's scheme [14] [15] [16]. This viscous term is nearly a laplacian, which is decomposed over each element. Then, we compute the viscosity of this term in order to dump the fastest wave.

In order to limit the degradation of the LW-PSI scheme, we use the pressure sensor designed by Jameson in 85 [14]

$$ps_{i,j} = min\left(ps_i, ps_j\right) \text{ with } ps_i = \frac{\mid p_j - p_i - \nabla p_i \cdot \overrightarrow{N_i N_j} \mid}{\mid p_j + p_i - \nabla p_i \cdot \overrightarrow{N_i N_j} \mid} \tag{39}$$

This pressure sensor helps us to add viscosity only near the shocks. In practise, the viscous term we add is

$$\Phi^i_{visc} = \left(r^1, r^2, r^3\right) \frac{1}{2 \sum\limits_{T/i \in T} V^T} \left(\sum_{T/i \in T} \sum_{j \neq i} \lambda_{i,j} \cdot \epsilon_{i,j} \cdot S^e \left(\nabla \check{W} \cdot \overrightarrow{N_i N_j} \right) \right) \tag{40}$$

with

$$\lambda_i = max\left[\mid \vec{\lambda}^1 \cdot \vec{n}_i \mid, \mid \vec{\lambda}^2 \cdot \vec{n}_i \mid, \mid \vec{\lambda}^3 \cdot \vec{n}_i \mid \right] \ , \ \lambda_{i,j} = \frac{\lambda_i + \lambda_j}{2} \tag{41}$$

$$\vec{\lambda}^1 = \chi \vec{n} + \frac{\chi}{\beta} \vec{s}, \ \vec{\lambda}^2 = \chi \vec{n} - \frac{\chi}{\beta} \vec{s}, \ \vec{\lambda}^3 = \frac{\chi}{\beta} \vec{t} \tag{42}$$

and

$$\epsilon_{i,j} = \min\left(1, k \ ps_{i,j}\right) \text{ with } k = 15 \tag{43}$$

5.4 The Roe linearization

Until now, it has been proceeded as if the Euler equations were linear. The extension of the fluctuation splitting method to non linear conservation laws is largely discussed in Paillère 95 [2] and the conclusion is that the linearisation $\mathcal{L}\left(\bar{Z}\right)$ [17] [18] has to be used as far as we have to get a constant approximation of whatever quantity.

We just recall here that this linearization is a generalisation of the Roe average. This linearisation is based on the assumption that the parameter vector $Z = \sqrt{\rho}\left(1, u, v, w, h\right)$ varies linearly over each element. This choice of Z is such that W and the fluxes F, G, H are quadratic in the components of Z and so the jacobians of these four quantities are linear in the components of Z.

6 The time-integration to the steady state

The explicit scheme used to compute Euler steady states has been presented. But our industrial constraints are such that explicit schemes are not fast enough. This is the reason why implicit schemes have to be used.

The way, chosen to obtain an implicit scheme, is discussed here.

The explicit scheme can be written as

$$W_i^{n+1} = W_i^n - \frac{\Delta t_i}{V_i} Res_i\left(W^n\right) \tag{44}$$

where $Res_i\left(U^n\right)$ is the residual which is affected to node i at the iteration n.

Any implicit scheme can be written as

$$W_i^{n+1} = W_i^n - \frac{\Delta t_i}{V_i} Res_i\left(W^{n+1}\right) \tag{45}$$

As far as we are concerned, a linearised implicit scheme is used. Thus, we write

$$Res_i\left(W^{n+1}\right) \simeq Res_i\left(W^n\right) + \frac{\partial Res_i}{\partial W}\left(W^n\right) \cdot \left(W^{n+1} - W^n\right) \tag{46}$$

where $\dfrac{\partial Res_i}{\partial U}$ is the jacobian matrix of Res_i

Finally, we use

$$W^{n+1} = W^n + \left(Id + \frac{\Delta t}{V}\frac{\partial Res}{\partial W}\left(W^n\right)\right)^{-1} \cdot \left(-\frac{\Delta t}{V} Res\left(W^n\right)\right) \tag{47}$$

where $\dfrac{\Delta t}{V}$ is a block diagonal matrix, whose each block is $\dfrac{\Delta t_i}{V_i} Id$.

Once more, we have to face our industrial constraints. As a matter of fact, we cannot store the matrix $Id + \dfrac{\Delta t}{V}\dfrac{\partial Res}{\partial W}\left(W^n\right)$ and inverse it for each iteration. Because we have to guaranty a low storage, we have to solve

$$y = \left(Id + \frac{\Delta t}{V}\frac{\partial Res}{\partial W}\left(W^n\right)\right)^{-1} \cdot \left(-\frac{\Delta t}{V} Res\left(W^n\right)\right) \tag{48}$$

at each iteration of the unsteady process.

The resolution of this linear system is the issue of the next section.

6.1 The resolution of the linear system of the implicit scheme

In order to solve this linear system, we use a GMRES iterative solver [19].

Until the end of this section, we note $A = Id + \frac{\Delta t}{V}\frac{\partial Res}{\partial W}(W^n)$ and thus we note the linear system $Ax = b$.

The use of GMRES solver requires computations of Ax and a preconditioner.

The difficult point in the computations of Ax are those of $\frac{\partial Res}{\partial W}(W^n)\ x$. In order to realize these computations, we use a software, designed by INRIA: Odyssee [20]. This software is able to perform automatic differentiation of FORTRAN subroutines: it generates the subroutine for the computation of $\frac{\partial Res}{\partial W}(W^n)\ x$ from the subroutine of $Res\,(W^n)$. With this software, we have been able to compute the $\frac{\partial Res}{\partial W}(W^n)\ x$ in a very precise way.

Concerning the other point, we use a left block diagonal preconditionner and the computation of this preconditionning matrix is also realised with Odyssee.

The last point we have to precise is the way we compute time-steps.

6.2 The time-stepping

Because our objective is to get an Euler steady state, we are allowed to use a local time-stepping. We discuss here the choice of Δt_i we made.

First of all, the PSI-scheme is positive under the CFL condition [2]

$$\Delta t_i \leq \min_l \left(\frac{S_i}{\sum_{T/i\in T} max\left(0, |\ \vec{\check{\lambda}}^l \cdot \vec{n}_i\right)} \right) \tag{49}$$

with

$$\vec{\check{\lambda}}^l = \check{u}\ \vec{\lambda}^l \tag{50}$$

This gives a first constraint for the choice of the time-step. But, for reasons of robustness, we choose a more restrictive time-step

$$\Delta t_i = f(\epsilon)\ \frac{S_i}{\sum_{T/i\in T} (\check{u} + \check{a})\ \ \| \vec{n}_i \| \max\left(1, \chi\left(1 + \frac{1}{\beta}\right)\right)} \tag{51}$$

where

$$\epsilon = \frac{1}{3\ S_i} \sum_{T/i\in T} S_T \frac{\epsilon_{i,j} + \epsilon_{i,k} + \epsilon_{i,l}}{3} \tag{52}$$

and

$$f(x) = \frac{\sqrt{4 + x^2} - x}{2} \tag{53}$$

We have used this function f after having studied the stability of the one dimensional Lax Wendroff scheme with our additionnal viscosity. This scheme can be written as

$$\underbrace{\frac{u_i^{n+1}-u_i^n}{\Delta t}+a\frac{u_{i+1}^n-u_{i-1}^n}{2\Delta x}-a^2\frac{\Delta t}{2\Delta x^2}\mathcal{D}\left(u^n\right)}_{Lax\ Wendroff}-\underbrace{\epsilon\frac{a}{2\Delta x}\mathcal{D}\left(u^n\right)}_{viscosity}=0 \tag{54}$$

with

$$\mathcal{D}\left(u^n\right)=u_{i+1}^n-2u_i^n+u_{i-1}^n \tag{55}$$

and where we have called in the two former equations ϵ the coefficient based upon the Jameson pressure sensor.

A classical method gives the following stability criterium

$$\frac{a\ \Delta t}{\Delta x}\leq\frac{\sqrt{4+\epsilon^2}-\epsilon}{2} \tag{56}$$

and so f.

Indeed, Δt_i is the time-step we use with the explicit version of the code. In the implicit one, we multiply this time step by a factor which is taken between 1 and 100.

The work we have made about the implicitation of the Lax Wendroff - PSI scheme was a very necessary one in order to obtain a robust code, and thus to envisage an industrial use of this scheme. Moreover, each of the components of this work are crucial in order to obtain such a code.

At this point of the paper, all the different aspects of our scheme have been exposed. We now focus our attention on the results we get with this scheme.

7 Numerical results

Several results are presented here, in order to show the capabilities of the code.

In order to be able to validate our results, we compare them to these we obtain with the Lax Wendroff scheme of Dassault Aviation. Until the end of this paper, we note LW-PSI the Lax Wendroff - PSI scheme and LX the reference Lax Wendroff scheme.

The scheme LX is not a matrix Lax Wendroff scheme as in the scheme LW-PSI. This scheme LX has been first introduced by Billey in 84 [21] and is a predictor - corrector scheme which can be written in two steps

$$\text{Step 1 (prediction):}\quad \tilde{W}(T)=\frac{1}{V^T}\left[\iint_T W^n\ dV-\alpha\Delta t_{pred}\iint_{\partial T}\vec{F}\left(W^n\right)\cdot\vec{n}\ dS\right] \tag{57}$$

and

$$\text{Step 2 (correction):}\quad \Phi_i=\beta_1\iiint_T^{*}\vec{F}(W)\cdot\vec{\nabla}\Phi_i+\beta_2\iiint_T^{**}\vec{F}(\tilde{W})\cdot\vec{\nabla}\Phi_i-\text{A.V.} \tag{58}$$

where $\int^*$ and $\int^{**}$ represent two different approximation to compute the integrals.

In the equation 58, the term A.V. is an additionnal viscosity term, which looks like the term we have introduced in section 5.3.

Before going on, we have to precise that the scheme LX is considered validated.

7.1 Subsonic wing

In this test case, we compute a subsonic flow over the ONERA M6 wing, at a free stream Mach number equal to $M_\infty = 0.2$, and with no incidence.

The mesh (figure 1) has 27499 nodes and 152096 tetrahedras.

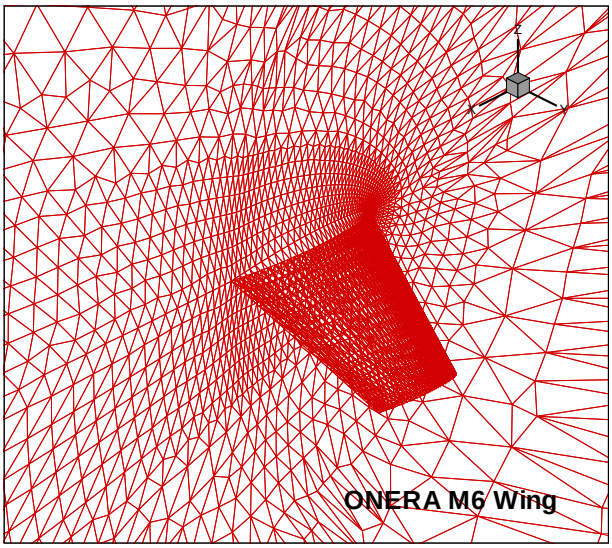

Fig. 1 : Partial view of the mesh of the ONERA M6 wing

First, we plot entropy deviation Σ along a profile, located at 60% on the wing span (figure 2). This Σ is defined by

$$\Sigma = \frac{p/p_\infty}{(\rho/\rho_\infty)^\gamma} - 1 \tag{59}$$

We recall that Σ is equal to zero in subsonic Euler computations.

We can notice that the scheme LW-PSI generates quite less numerical entropy than the scheme LX. This is illustrated by figure 3 where absolute value of Σ is plotted over the wing. We point out the difference of numerical entropy at the stagnation point (figure 2).

These more accurate entropy deviation allow to compute drags more precisely. In deed, in this test case, the drag is theoretically null and the computed drag is ten times less important with the scheme LW-PSI than with the scheme LX.

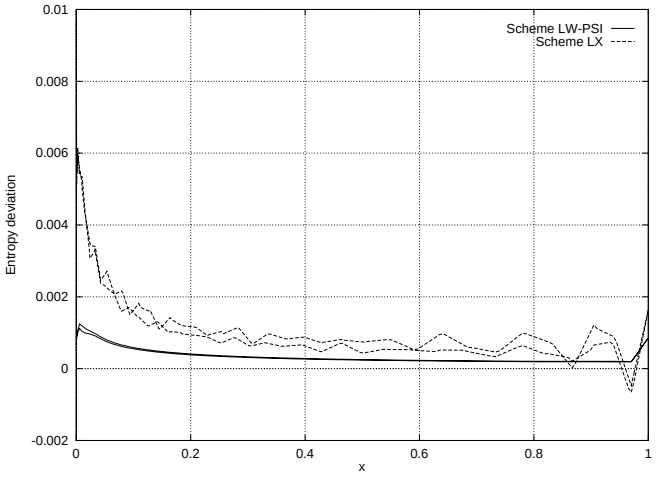

Fig. 2 : Comparison of Σ along a profile

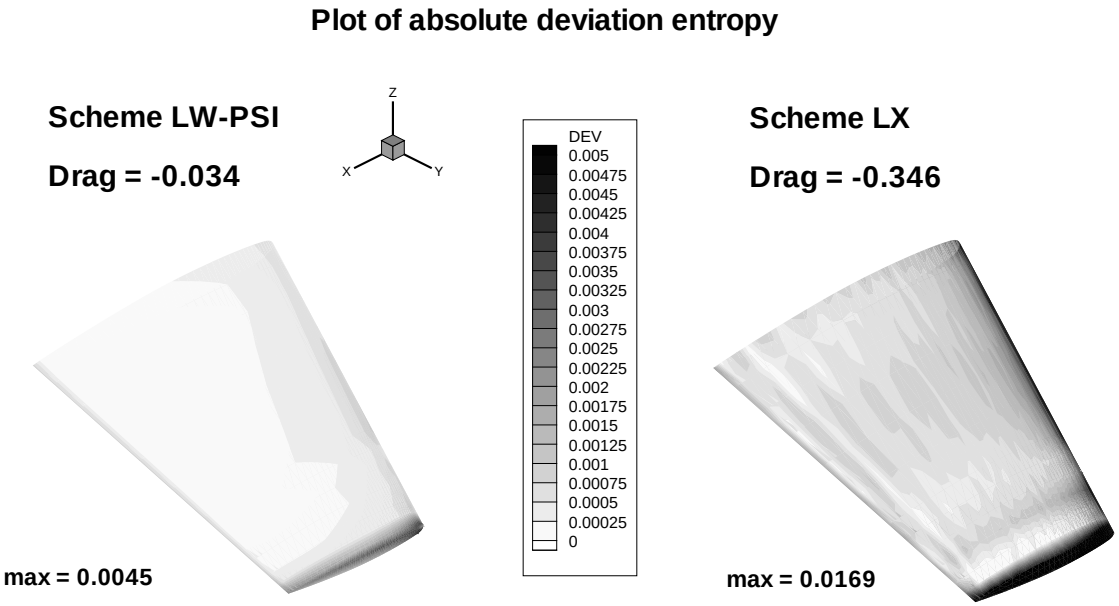

Fig. 3 : Comparison of absolute entropy deviation

7.2 Transonic wing

After having computed a subsonic flow over the ONERA M6 wing (section 7.1), we now investigate the capacities of the scheme LW-PSI to compute a transonic flow.

We use the same mesh as in section 7.1, and we take $M_\infty = 0.88$ and 6° for the incidence.

We choose to plot two quantities along the wing at the profile located at 60% of the span from the symmetry plane. These two quantities are the pressure coefficient C_p and entropy deviation Σ.

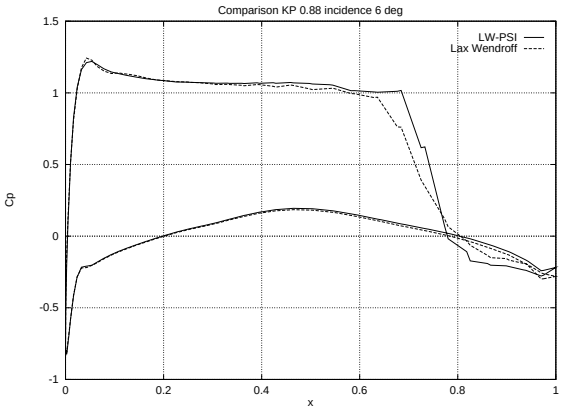

Fig. 4 : Comparison of C_p along a profile

The C_p distributions (figure 4) show that the scheme LW-PSI allow a more precise location of the shock than the scheme LX. Besides, we can notice that oscillations have been reduced near the shock, thanks to the additionnal viscous term we have introduced at section 5.3.

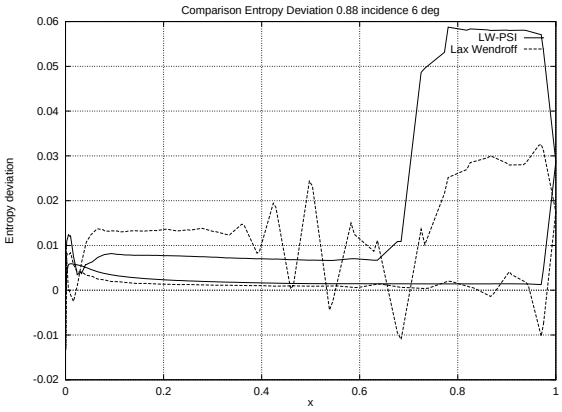

Fig. 5 : Comparison of Σ along a profile

The Σ distributions (figure 5) show that entropy distributions are significantly more precise with the scheme LW-PSI than with the scheme LX. This accuracy is certainly provided by the formulation of the scheme LW-PSI because this formulation takes into account the conservation of the entropy along streamlines.

We plot now the Mach number distributions along the same profile.

The Mach number distributions (figure 6) show that the scheme LW-PSI has a less viscous behavior than the scheme LX since Mach numbers are more important for the scheme LW-PSI than the scheme LX.

We can notice that the schock wave is stronger for the LW-PSI scheme. The C_p and Mach number distributions show no oscillations around the schock, but non physical spurious oscillations

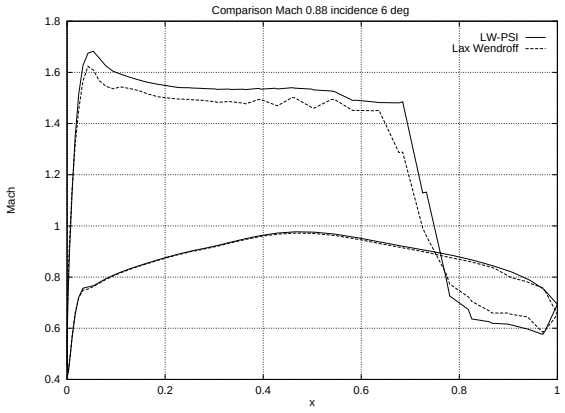

Fig. 6 : Comparison of Mach number along a profile

can be observed on the Σ distribution of the LX scheme although the expectable behavior is obtained with the LW-PSI scheme.

7.3 Low Mach cylinder

In this test case, we compute a flow over a cylinder with a very low Mach number, $M_\infty = 0.01$. Our aim is to show the ability of the scheme LW-PSI to compute nearly uncompressible flows.

We use a two dimensional mesh, with 11880 nodes and 23572 elements.

In figure 7, we plot pressure iso-lines for the flows computed by the two different schemes (LW-PSI and LX). We compare these iso-lines with those of the analytical incompressible flow for the same Mach number. Indeed, for such a low Mach number flow, the solution is nearly incompressible.

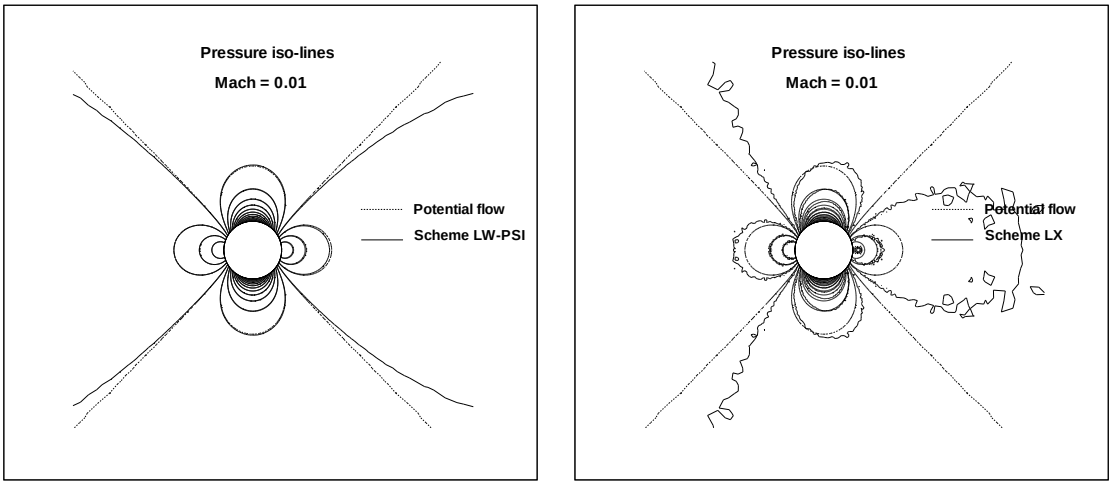

Fig. 7 : Pressure iso-lines for schemes LW-PSI (left) and LX (right)

This comparison (figure 7) show that the behavior of the scheme LW-PSI is quite good for low Mach number flows although the scheme LX has a poor behavior for such flows. This is likely due to the use of the van Leer-Lee-Roe matrix in the hyperbolic elliptic decomposition.

Moreover, the two symmetry planes are captured for the LW-PSI flow.

7.4 Subsonic zero-lift aircraft

In this last test case, we compute the flow over a generic aircraft. We take $M_\infty = 0.3$, in order to have a subsonic flow and thus no wave drag. Besides, we select the incidence of the flow such that the lift is null and therefore the vortex drag. Thus, the total drag computed with this inviscid code has to be null.

We use a mesh with 45387 nodes and 255944 tetrahedras. The simulation includes the fuselage, wings, stabilizers, nacelles and pylones.

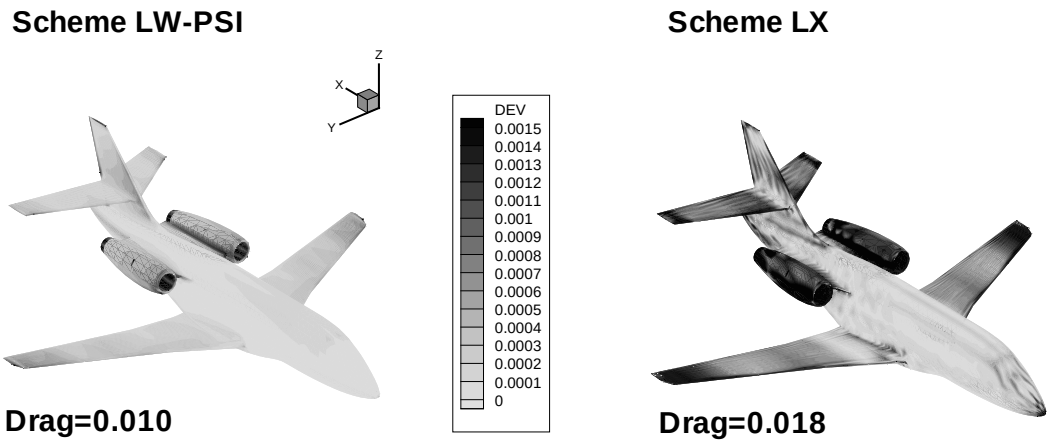

Fig. 8 : Absolute Σ over a trimmed aircraft

We plot the absolute entropy deviation over the aircraft (figure 8). As in section 7.1, we can confirm that the scheme LW-PSI generates quite less entropy than the scheme LX. However, the computed drag is only 40% lower with the scheme LW-PSI than with the scheme LX. This is due to the poor quality of the mesh in the neighbourhood of the nacelles.

8 Concluding remarks

We have obtained a code which allows Euler computations over a large Mach number range since it is good for $M_\infty = 0.01$ and we have made correct three dimensional computations for $M_\infty = 2$. In order to compute nearly hypersonic flows, it will be necessary to extend this scheme to the Euler equations with chemistery, as it has been done by Descamps and al. [22]

for the Osher scheme of Dassault Aviation.

The accuracy of the code allows more precise drag computations and more accurate shocks locations, as it has been shown in sections 7.1 and 7.4.

At this stage, we are satisfied of the additionnal viscous term (section 5.3) we have added to the initial scheme of Paillère [2]. However we think that this term is not optimal because no theoritical study have been realised upon this term and thus the added viscosity may not be optimal.

This code is precise and robust enough to allow an industrial use of this code although we have to acknowledge that this robustness and this accuracy is achieved at the expense of a higher cpu cost: at this step of the development of fluctuation splitting methods, we still have to make a choice between accuracy (scheme LW-PSI) and speed (scheme LX).

9 Acknowledgments

We would like to thank P.L.Roe, R.Abgrall, H.Paillère, H.Deconinck, E.van der Weide for their fruitful discussions on fluctuation splitting schemes and Q.V.Dinh, C.Sevin, T.Fanion for their collaboration in the implicitation of the scheme which is discussed in this paper.

Special thanks are due to M.Mallet, B.Stoufflet and M.Ravachol for their useful remarks and J.Francescatto for his advices.

We thank the European Commission for supporting this work.

References

[1] **H.Deconinck, H.Paillere, R.Struijs and P.L.Roe**, Multidimensional upwind schemes based on fluctuation-splitting for systems of conservation laws, *Journal of Computational Mechanics, 11(5/6): 323-340, 1993.*

[2] **H.Paillère**, Multidimensional Upwind Residual Distribution Schemes for the Euler and Navier-Stokes Equations on Unstructured Grids, *thèse de l'Université Libre de Bruxelles, 1995.*

[3] **A.Bonfiglioli, E. van der Weide and H.Deconinck**, Study of 3D hypersonic flow using unstructured grid solvers based on multidimensional upwinding, *von Karman Institute for Fluid Dynamics, 1996.*

[4] **P.L.Roe**, Discrete models for the numerical analysis of time-dependent multidimensional gas dynamics, *Journal of Computational Physics, 63, 1986.*

[5] **H.Deconinck, Ch. Hirsch and J.Peuteman**, Characteristic decomposition methods for the multidimensional Euler equations, *Lecture Notes in Physics, volume 264, Springer-Verlag, 1986.*

[6] **B.van Leer, W.T.Lee and P.Roe**, Characteristic Time-Stepping or Local Preconditionning of the Euler Equations,*AIAA 10th Computational Fluid Dynamics Conference 1991, AIAA-91-1552-CP.*

[7] **P.L.Roe**, Linear advection schemes on triangular meshes, *Technical report, Cranfield Institute of Technology, November 1987, CoA 8720.*

[8] **M.Rudgyard**, Cell-vertex methods for steady inviscid flow, *VKI LS 1993-04, Computational Fluid Dynamics, 1993*

[9] **H.Paillère, H.Deconinck and E. van der Weide**, Upwind residual distribution methods for compressible flow: an alternative to finite volume and finite element methods, *von Karman Institute for Fluid Dynamics, presented at the 28th CFD Lecture Series, March 1997.*

[10] **R.Strujis, H.Deconinck and P.L.Roe**, Fluctuation Splitting Schemes for the 2D Euler Equations. *VKI LS 1991-01, Computational Fluid Dynamics, 1991.*

[11] **D.Sidilkover and P.L.Roe**, Unification of some advection schemes in two dimensions, *Technical Report 95-10, ICASE, 1995*

[12] **D.Sidilkover**, Multidimensional upwinding and multigrid, *1995 12th AIAA CFD Conference, San Diego, Paper 95-1759.*

[13] **D.Sidilkover**, Numerical solution to steady-state problems with discontinuities, *PhD thesis, The Weizmann Institute of science, Rehovot, Israel, 1989.*

[14] **A.Jameson and W.Schmidt**, Some recent developments in numerical methods for transonic flows, *Computer Methods in Applied Mechanics and Engineering 51 (1985) 467-493, North Holland.*

[15] **J.Peraire, J.Peiro, L.Formaggia, K.Morgan and O.C.Zienkiewicz**, *Finite Element Euler Computations in Three Dimensions, Int. J. Numerical Methods in Engineering, vol 26, 2135-2159 (1988).*

[16] **V.Selmin**, A Multistage Method for the Solution of the Euler Equations on Unstructured Grids,*Proceedings of the fifth International Symposium on Numerical Methods in Engineering.*

[17] **R.Strujis, H.Deconinck, P.De Palma, P.L.Roe and K.G.Powell**, Progress on multidimensional upwind Euler solvers for unstructured grids, *AIAA-91-1550, 1991.*

[18] **H.Deconinck, P.L.Roe, and R.Struijs**, a Multidimensional generalization of Roe's flux difference splitter for the Euler equations, *Journal of Computers and Fluids, 22(2/3]:215-222,1993.*

[19] **Y.Saad**, Krylov subspace methods on supercomputers, *S.I.A.M., Vol 10, No. 6, pages 1200-1232, Novembre 1989.*

[20] **C.Faure and Y.Papegay**, Odyssée Version 1.6 The User's Reference Manual, *Rapport INRIA 0211, Novembre 1997.*

[21] **V.Billey**, Résolution des équations d'Euler par des méthodes d'éléments finis, application aux écoulements 3D de l'aérodyamique, *Thèse de l'Université Pierre et Marie Curie Paris VI, 1984.*

[22] **A.Descamps, M.P.Leclerc and B.Stoufflet**, Two and three dimensional compressible fluid flow computations with unstructured grids, *Ninth International Conference on Computing Methods in Applied Sciences and Engineering, January 1990.*